Historic England

Research Report Series 26/2023

CASTILLY HENGE, LUXULYAN, CORNWALL

Report on Geophysical Surveys, February 2022

Neil Linford and Andrew Payne

Geophysics

CASTILLY HENGE, LUXULYAN, CORNWALL

Report on Geophysical Surveys, February 2022

Neil Linford and Andrew Payne

Castilly Henge
Luxulyan
Cornwall

NGR: SX 03111 62755

Print: ISSN 2398-3841
Online: ISSN 2059-4453

The Research Report Series incorporates reports by Historic England's expert teams, their predecessors and other researchers. Many Research Reports are interim, to make available the results of specialist investigations in advance of full publication. Although subject to internal quality assurance, they are not usually refereed externally and their conclusions may sometimes have to be modified in the light of information not available at the time of the investigation. Where no final project report is available, readers should consult the author before citing these reports.

For more information email Res.reports@HistoricEngland.org.uk or write to:

Historic England
Fort Cumberland
Fort Cumberland Road
Eastney
Portsmouth PO4 9LD

Opinions expressed in Research Reports are those of the author(s) and are not necessarily those of Historic England.

Summary

Ground Penetrating Radar (GPR), magnetic and earth resistance surveys were conducted at Castilly Henge, Luxulyan as part of a project to support ongoing work to remove the monument from the Heritage at Risk (HAR) register. Vehicle towed GPR survey (0.6ha) and earth resistance survey (0.1ha) revealed an eccentric ovoid arrangement of internal pits within the henge ditch, with a possible indication of recumbent stones. The response to the pits was less well defined in the magnetic data (0.4ha) and few significant anomalies were found with any of the techniques to the north of the henge beyond responses to a ferrous gas pipe, the underlying geology and former field boundary known from the historic mapping.

Contributors

The geophysical fieldwork was conducted by Neil Linford and Andrew Payne.

Acknowledgements

The authors are grateful to the landowner for allowing access to the site for the survey to be conducted, and to the local volunteers for all their hard work clearing vegetation from the site.

Archive location

Fort Cumberland, Portsmouth.

Date of survey/research/investigation

The fieldwork was conducted between the 24th to 26th February 2022 and the report completed on 11th May 2023. The cover image shows a monochrome image of the southern entrance to the henge in the low winter light (photograph taken by N Linford).

Contact details

Dr Neil Linford, Geophysics team, Historic England, Fort Cumberland, Fort Cumberland Road, Eastney, Portsmouth PO4 9LD (02392 856761, neil.linford@historicengland.org.uk).

Contents

Introduction 1

Method 2

- Ground Penetrating Radar survey 2
- Magnetometer survey.. 3
- Earth resistance survey 3

Results 4

- Ground Penetrating Radar survey 4
- Magnetometer survey.. 5
- Earth resistance survey 5

Conclusions.. 6

List of Enclosed Figures 8

References.. 10

Introduction

Ground Penetrating Radar (GPR), magnetic and earth resistance surveys were conducted at Castilly Henge, Luxulyan, Cornwall, as part of a wider non-invasive study of the site, undertaken in support of work to remove Castilly henge from the Heritage at Risk (HAR) register. Historic England's (HE) Archaeological Investigation Team (AIT) has conducted a level 3 analytical earthwork survey, a contextual Aerial Investigation and Mapping (AIM) study of its immediate environs (Bayer and Small forthcoming). together with a geophysical survey of the scheduled monument reported on here. The geophysical survey was preceded by fencing and bracken management works undertaken as part of the Cornwall Archaeology Unit's (CAU) Monument Management Scheme (MMS), and it is hoped that the combined non-invasive investigation of the monument will provide a basis for the future management and presentation of the site (Newsome *et al.* 2021).

The Castilly henge scheduled monument (NHLE 1006684) is slightly under 1ha in extent and comprises the earthworks of an extant late Neolithic henge monument, thought to have been subsequently modified as a medieval playing place (plen-an-gwarry), and as a suggested civil war battery. The site sits at the north-east corner of a group of small, regular rectilinear fields, typical of 'recently enclosed land' in Cornwall, and likely to reflect early 19th century enclosure of the surrounding downland. Some irregularities in the earthworks may be the result of removing material for 'manuring' this new intake. Henge monuments are rare in Cornwall and Devon, Castilly being one of only 3 known examples in Cornwall. A generalised earthwork survey of the site was carried out alongside small-scale excavation in the 1960s (Thomas 1964; Newsome *et al.* 2021).

The site lies over metamorphosed Lower Devonian calcareous slate, grit and thin limestone of the Meadfoot Beds where loamy permeable upland soils of the HAFREN (654a) Association are recorded (Geological Survey of Great Britain (England and Wales) 1982; Soil Survey of England and Wales 1983). Surface conditions were generally down to rough pasture, with vegetation largely cleared by the volunteers from the monument itself with some inaccessible areas due piles of green waste awaiting removal from the site. Weather conditions were generally cold but dry throughout the field work.

Method

Ground Penetrating Radar survey

A 3d-Radar MkIV GeoScope Continuous Wave Step Frequency (CWSF) Ground Penetrating Radar (GPR) system was used to conduct the survey collecting data with a multi-element DXG1820 vehicle towed, ground coupled antenna array (Linford *et al.* 2010; Eide *et al.* 2018). A roving Trimble R8s Global Navigation Satellite System (GNSS) receiver was mounted on the GPR antenna array, that together with a second R8s base station was used to provide continuous positional control for the survey collected along the instrument swaths shown on Figure 1. The GNSS base station receiver was adjusted to the National Grid Transformation OSTN15 using the Trimble VRS Now Network RTK delivery service. This uses the Ordnance Survey's GNSS correction network (OSNet) and gives a stated accuracy of 0.01-0.015m per point with vertical accuracy being half as precise.

Data were acquired at a 0.075m x 0.075m sample interval across a continuous wave stepped frequency range from 40MHz to 2.99GHz in 4MHz increments using a dwell time of 2ms. A single antenna element was monitored continuously to ensure data quality during acquisition together with automated processing software to produce real time amplitude time slice representations of the data as each successive instrument swath was recorded in the field (Linford 2013).

Post-acquisition processing involved conversion of the raw data to time-domain profiles (through a time window of 0 to 75ns), adjustment of time-zero to coincide with the true ground surface, background and noise removal, and the application of a suitable gain function to enhance late arrivals. Representative profiles from the full GPR survey data set are shown on Figure 7. To aid visualisation amplitude time slices were created from the entire data set by averaging data within successive 2.5ns (two-way travel time) windows (e.g. Linford 2004). An average sub-surface velocity of 0.104m/ns was assumed following constant velocity tests on the data and was used as the velocity field for the time to estimated depth conversion. Each of the resulting time slices therefore represents the variation of reflection strength through successive ~0.13m intervals from the ground surface, shown as individual greyscale images in Figures 2, 8, 9 and 10. Further details of both the frequency and time domain algorithms developed for processing this data can be found in Sala and Linford (2012).

Due to the size of the resultant data set a semi-automated algorithm has been employed to extract the vector outline of significant anomalies shown on Figure 13. The algorithm uses edge detection to identify bounded regions followed by a morphological classification based on the size and shape of the extracted anomalies. For example, the location of possible pits is made by selecting small, sub circular anomalies from the data set (Linford and Linford 2017).

Magnetometer survey

A series of 30m grids were established in the interior of the henge and field to the north with a Trimble R8s Global Navigation Satellite System (GNSS) and surveyed using a Bartington Grad 601 dual fluxgate gradiometer (Figure 3). In the henge measurements were recorded at 0.25 m intervals along parallel traverses separated by 0.5m achieved by repeating each grid with a 0.5m offset to the initial traverses. A coarser 1.0m traverse separation was used in the external area of magnetometer coverage. Post-acquisition, the median value of each traverse was subtracted from all measurements on that traverse (Zero Median Traverse) to correct for heading errors and instrument drift. A linear greyscale image of the magnetometer data is presented in Figures 4 and 5 superimposed on the OS base map. A trace plot and a linear greyscale image of the minimally processed data are shown on Figure 11.

Earth resistance survey

Two partial 30m grids (Figure 3) were established in the interior of the henge with a Trimble R8s Global Navigation Satellite System (GNSS) and surveyed using a Geoscan RM85 resistance meter with an internal multiplexer and a PA5 frame with three electrodes in the parallel Twin-Electrode configuration. This arrangement allowed two separate surveys, with electrode separations of 0.5m and 1.0m, to be collected simultaneously. The 0.5m electrode separation coverage was designed to detect near-surface anomalies in the upper 0.5m of the subsurface whilst the 1.0m separation survey allowed anomalies to a depth of about 1-1.25m to be detected. For the 0.5m electrode separation survey readings were taken at a density of 1.0m x 0.5m whilst for the 1.0m separation survey they were taken at a density of 1.0m x 1.0m.

Extreme values caused by high contact resistance were suppressed from both datasets using an adaptive thresholding median filter with radius 1m (Scollar et al. 1990), and then processed using a high-pass filter to enhance anomalies 1-2m in width while simultaneously suppressing measurement noise. The results for the near-surface 0.5m electrode separation survey following the processing described above are depicted as a linear greyscale image in Figure 6 superimposed on the base OS map data. Figure 12 shows the minimally processed data from both the 0.5m and 1.0m electrode separation data, presented as trace plots and linear greyscale images, together with linear greyscale images of the processed datasets following the application of a high-pass filter.

Results

Ground Penetrating Radar survey

A graphical summary of the significant GPR anomalies, [**gpr1-16**] discussed in the following text, superimposed on the base OS map data, is provided in Figure 13.

The near-surface data between 0.0 and 5.0ns (0.0 to 0.26m) is heavily influenced by vehicle ruts [**gpr1**] associated with the recent vegetation clearance [**gpr2**], together with possible mole runs [**gpr3**] both within and immediately outside the henge. A high amplitude response [**gpr4**] has also been recorded over the marginal vegetation found on lower lying, wetter ground to the north. Deeper lying, high amplitude linear striations [**gpr5**] between 7.5 and 20.0ns (0.39 to 1.04m) are found within an east west low amplitude band, possibly associated with the trend of the underlying metamorphic Bovisand Formation slate and sandstone.

Two large services [**gpr6**] and [**gpr7**] are found to the north of the site, presumably one or both of these are related to the known gas main. Both services fall from west to east across the site, with [**gpr6**] visible from 22.5ns (1.17m) deviating slightly to the south after entering from the road beneath the field gate, and [**gpr7**] found from 40.0ns (2.08m) parallel to the northern field boundary. A former field boundary [**gpr8**] appears initially as a low-amplitude trench from 12.5ns (0.65m) entering from the north of the survey area continuing south east just avoiding the henge (OS Historic County Mapping Series: Cornwall 1907 Epoch 2). In the deeper lying data, from 22.5ns (1.17m) onwards, [**gpr8**] appears as a parallel high-amplitude anomaly for a short length to the north, continuing as linear response across the site to the south. It is possible that this may represent either an original walled field boundary or, perhaps, reuse for an agricultural water supply. The spur of the original field boundary to the west is just visible as a high-amplitude, parallel linear anomaly [**gpr9**].

Parallel high-amplitude anomalies [**gpr10**] are found between 7.5 and 20.0ns (0.39 to 1.04m) within the interior of the henge in the vicinity of the southern entrance. However, the significance of [**gpr10**] is difficult to ascertain as there are no associated anomalies in either the magnetic or earth resistance datasets. Of much greater interest are a group of discrete high-amplitude anomalies [**gpr11-16**] found between 12.5 and 25.0ns (0.65 to 1.3m) arranged in an ovoid arc. To the east of the henge the individual anomalies [**gpr11-**

14] are more rectilinear in form, with a long axis of approximately 0.9m by 2-3m, and do not appear to share the apparent orientation of the underlying geology [**gpr5**]. The morphology of [**gpr11-16**], considered as both individual anomalies and the form of the group as a whole, suggests an incomplete arc of pits or, perhaps, buried stones.

Magnetometer survey

A graphical summary of significant magnetic anomalies [**m1-12**] discussed in the following text superimposed on the base OS mapping data is provided in Figure 14.

The bulk of the henge interior is characterised by a relatively quiet and undisturbed magnetic response. A strong ferrous response [**m1**] is located in the north-east quadrant of the henge, possibly of relatively recent origin, although it may, perhaps, be associated with either the suggested English Civil War gun battery known at the site (List Entry 1006684) or activity immediately to the north of the previous excavation trenches (Thomas 1964, Fig 1). A weaker anomaly [**m2**], to the west just inside the north entrance to the henge, may represent a more significant pit-type response, localised area of burning or, perhaps, a later intrusion again possibly associated with the previous excavation. A number of weak linear negative anomalies with no obvious pattern within the henge may, perhaps, relate to minor variations in surface topography such as modern vehicle tracks.

Highly tentative negative anomalies [**m3-8**] are just visible above the noise threshold to the south of the henge, forming an arc that corresponds with a similar arrangement of discrete high amplitude GPR responses [**gpr11-16**] and low resistance pits [**r2-7**]. The weak magnitude of response of [**m3-8**] precludes a more confident interpretation without the evidence from the other two survey methods.

Data to the north of the henge is dominated by strong ferrous disturbance from the modern services [**m9**] and [**m10**], including a gas main that that totally obscures the identification of any significant archaeological responses. The previous field boundary known from historic mapping has been detected as a weakly defined ditch-type anomaly [**m11**], passing immediately to the east of the henge (OS Historic County Mapping Series: Cornwall 1907 Epoch 2, cf [**gpr8**]). A negative anomaly [**m12**] appears to follow the course of the north bank of the henge, presumably constructed from the stone excavated from the ditch, where it falls just within the magnetometer survey coverage.

Earth resistance survey

A graphical summary of significant earth resistance anomalies [**r1-18**] discussed in the following text superimposed on the base OS mapping data is provided in Figure 14.

A high resistance response [**r1**] is found inside the oval platform forming the henge interior coinciding with the inner scarp of the rock-cut ditch but absent at the infilled northern entrance. The background resistance is significantly lower away from the edge of the platform where an arc of equally spaced pit-type anomalies [**r2-7**], each approximately 1.5m in diameter, are found to the south of the henge and are best resolved in the high-pass filtered near-surface data (Figure 12(C)). Anomalies [**r2-7**] are suggestive of a similar eccentric ovoid arrangement of internal pits known from aerial photography over the ploughed out henge at Bow on Dartmoor (Griffiths 1985).

There is no evidence for the continuation of the pattern of pits in the northern portion of the henge and while they may not extend into this area more subtle anomalies could be difficult to detect here due to disruption by later activity, for example the broader polygonal low resistance response [**r8**] associated with the recent vegetation clearance. Immediately south of [**r8**] a weakly defined circular area of raised resistance [**r9**], approximately 7.5m in diameter, appears connected with linear anomalies to the south [**r10**] and east [**r11**]. It is difficult to fully interpret the archaeological significance of [**r9-11**] or whether they are associated with more recent activity.

Further low resistance pit-type anomalies to the south may be present at [**r12**] and [**r13**], within the weak circular area of raised resistance [**r9**], and at [**r14**] and [**r15**], but these do not appear to form part of the main arc [**r2-7**]. The southern and central portions of the henge interior also demonstrate broad areas of slightly lower background resistance [**r16-18**], that may relate to slightly deeper deposits of topsoil or variations in geology and drainage.

Conclusions

Despite the ferrous interference from the gas main obscuring results from the magnetic survey to the north of the site, all three techniques were successfully applied within the interior of the henge. The most significant anomalies revealed within the henge were an eccentric ovoid arrangement of pits in the earth resistance data that partially correlate with a series of high amplitude GPR responses. This is certainly suggestive of a Neolithic henge with the internal arrangement of pits associated with significant deposits from an approximate depth of 0.65m. It is possible from the size and relative location of the GPR anomalies that these may even represent recumbent stones, originally set within the pits identified by the earth resistance survey. However, such an interpretation remains questionable given the previous excavation data that suggested the absence of any internal features within the henge. It is, of course, possible that the excavation trenches narrowly missed the location of the subsequently revealed anomalies, although Trench 6a would appear to coincide with both [**r7**] and [**gpr12**] (Thomas 1964, Fig 1.). Few significant anomalies were found to the north of the henge beyond the response to the underlying geology and former field boundary known from the historic mapping.

List of Enclosed Figures

Figure 1: Location of the GPR instrument swaths superimposed over the base OS mapping data (1:750).

Figure 2: Greyscale image of the GPR amplitude time slice from between 15.0 and 17.5ns (0.78 – 0.91m) superimposed over the base OS mapping data. The location of representative GPR profiles shown on Figure 7 are also indicated (1:750).

Figure 3: Location of the fluxgate magnetometer and earth resistance survey grids superimposed over the base OS mapping data (1:750).

Figure 4: Linear greyscale image of the fluxgate magnetometer superimposed over the base OS mapping data (1:750).

Figure 5: Linear greyscale image of the fluxgate magnetometer from the henge interior superimposed over the base OS mapping data (1:500).

Figure 6: Linear greyscale image of the 0.5m mobile probe spacing earth resistance data from the henge interior superimposed over the base OS mapping data (1:500).

Figure 7: Representative topographically corrected profiles from the GPR survey shown as greyscale images with annotation denoting significant anomalies. The location of the selected profiles can be found on Figures 1, 2 and 13.

Figure 8: GPR amplitude time slices between 0.0 and 20.0ns (0.0 to 1.04m) (1:1250).

Figure 9: GPR amplitude time slices between 20.0 and 40.0ns (1.04 to 2.08m) (1:1250).

Figure 10: GPR amplitude time slices between 40.0 and 60.0ns (2.08 to 3.12m) (1:1250).

Figure 11: (A) Trace plot of range truncated and (B) linear greyscale image of the minimally processed fluxgate magnetometer data (1:750).

Figure 12: (A) Trace plot, (B) linear greyscale image of the minimally processed 0.5m mobile earth resistance data, together with (C) a linear greyscale image following the application of a high-pass filtered. (D), (E) and (F) show the same representations for the 1.0m mobile probe spacing data (1:500).

Figure 13: Graphical summary of significant GPR superimposed over the base OS mapping (1:750).

Figure 14: Graphical summary of significant fluxgate magnetometer and earth resistance anomalies superimposed over the base OS mapping (1:750).

References

Bayer, O and Small, F forthcoming *'CASTILLY HENGE, LUXULYAN, CORNWALL Report on Analytical Earthwork and Aerial Surveys'*. Historic England Research Report.

Eide, E, Linford, N, Persico, R and Sala, J 2018 'Advanced SFCW GPR systems' *in* Persico, R, Piro, S and Linford, N (eds), *Innovation in Near-Surface Geophysics Instrumentation, Application, and Data Processing Methods* Amsterdam: Elsevier, 253-285.

Geological Survey of Great Britain (England and Wales) 1982 Bodmin, England and Wales Sheet 347, Solid and Drift edition. 1:50000 series., Ordnance Survey, Chessington, Surrey.

Griffiths, F M 1985 'Some newly discovered ritual monuments in Devon'. *Proceedings of the Prehistoric Society*, **51** (1), 310-15.

Linford, N 2004 'From Hypocaust to Hyperbola: Ground Penetrating Radar surveys over mainly Roman remains in the U.K.'. *Archaeological Prospection*, **11** (4), 237-246.

Linford, N 2013. *Rapid processing of GPR time slices for data visualisation during field acquisition*. In Neubauer, W, Trinks, I, Salisbury, R and Einwogerer, C (Editors), Archaeological Prospection, Proceedings of the 10th International Conference, May 29th - June 2nd 2013 2013 (Vienna: Austrian Academy of Sciences Press). 176-78.

Linford, N and Linford, P 2017. *The application of semi-automated vector identification to large scale archaeological data sets considering anomaly morphology*. In Jennings, B, Gaffney, C, Sparrow, T and Gaffney, S (Editors), 12th International Conference of Archaeological Prospection, 12-16th September 2017 2017 (Bradford: Archaeopress Archaeology). 138-9.

Linford, N, Linford, P, Martin, L and Payne, A 2010 'Stepped-frequency GPR survey with a multi-element array antenna: Results from field application on archaeological sites'. *Archaeological Prospection*, **17** (3), 187-198.

Newsome, S, Oakley, M and Bayer, O 2021 Project Design Castilly Henge, Luxulyan, Cornwall, Internal Project Design, Historic England.

Sala, J and Linford, N 2012 ' Processing stepped frequency continuous wave GPR systems to obtain maximum value from archaeological data sets '. *Near Surface Geophysics*, **10** (1), 3-10.

Scollar, I, Tabbagh, A, Hesse, A and Herzog, I 1990 *Archaeological Prospecting and Remote Sensing*. Topics in Remote Sensing. Cambridge, Cambridge University Press.

Soil Survey of England and Wales 1983 Soils of England and Wales: Sheet 5 - South West England, 1:250,000 soil map. Harpenden, Lawes Agricultural Trust.

Thomas, C 1964 'The Society's 1962 Excavations: The Henge at Castilly, Lanivet'. *Cornish Archaeology*, **3**, 3-14.

CASTILLY HENGE, LUXULYAN, CORNWALL

Figure 1

Location of GPR instrument swaths, January 2022

SX0362

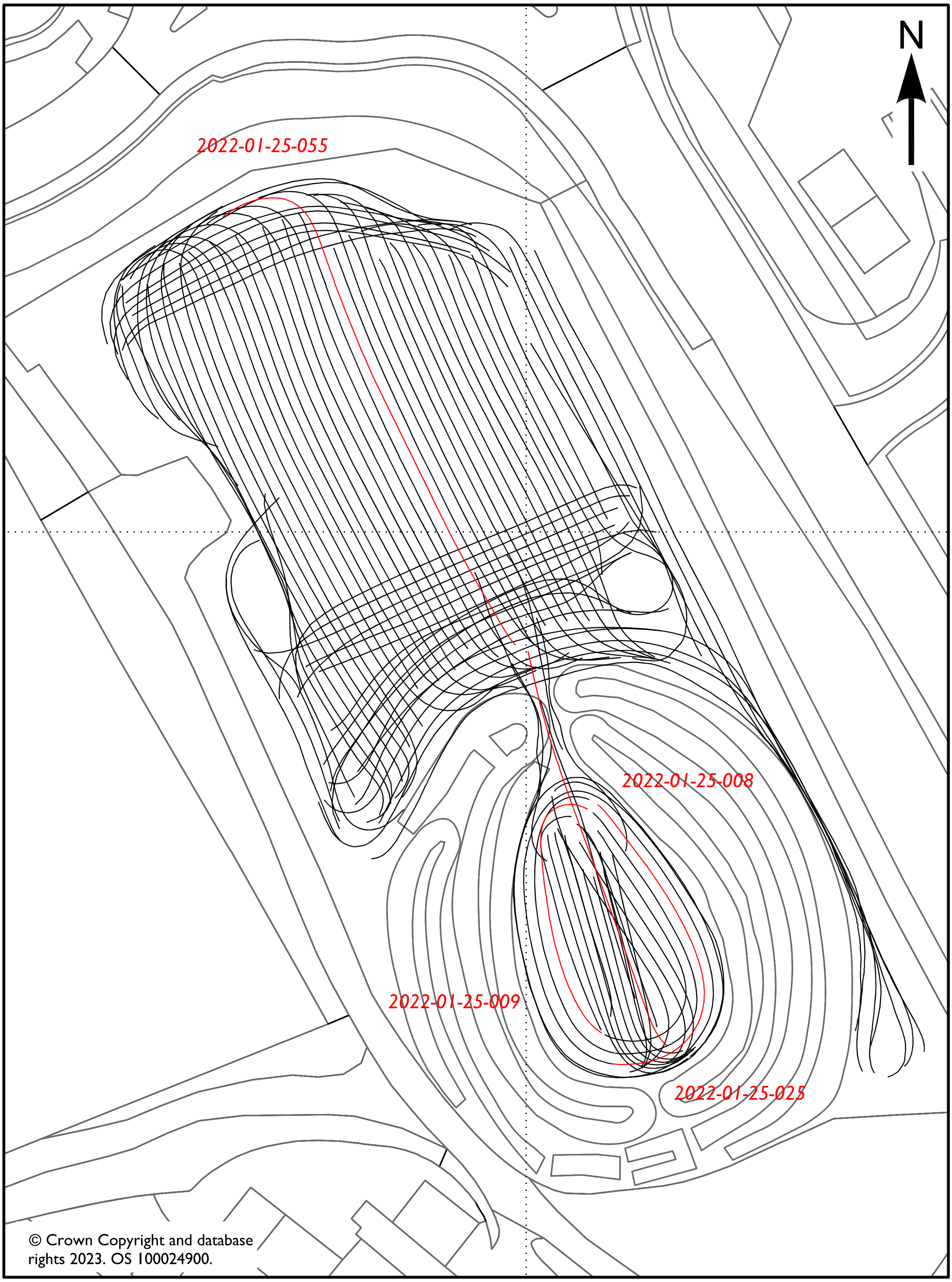

0 30m

1:750

Ground Penetrating Radar survey swaths

2022-01-25-001 Location of selected GPR profiles shown on Figure 7

Geophysics Team 2023

Historic England

CASTILLY HENGE, LUXULYAN, CORNWALL

Figure 2

GPR amplitude time slice between 15.0 and 17.5ns (0.78 to 0.91m), January 2022

SX0362

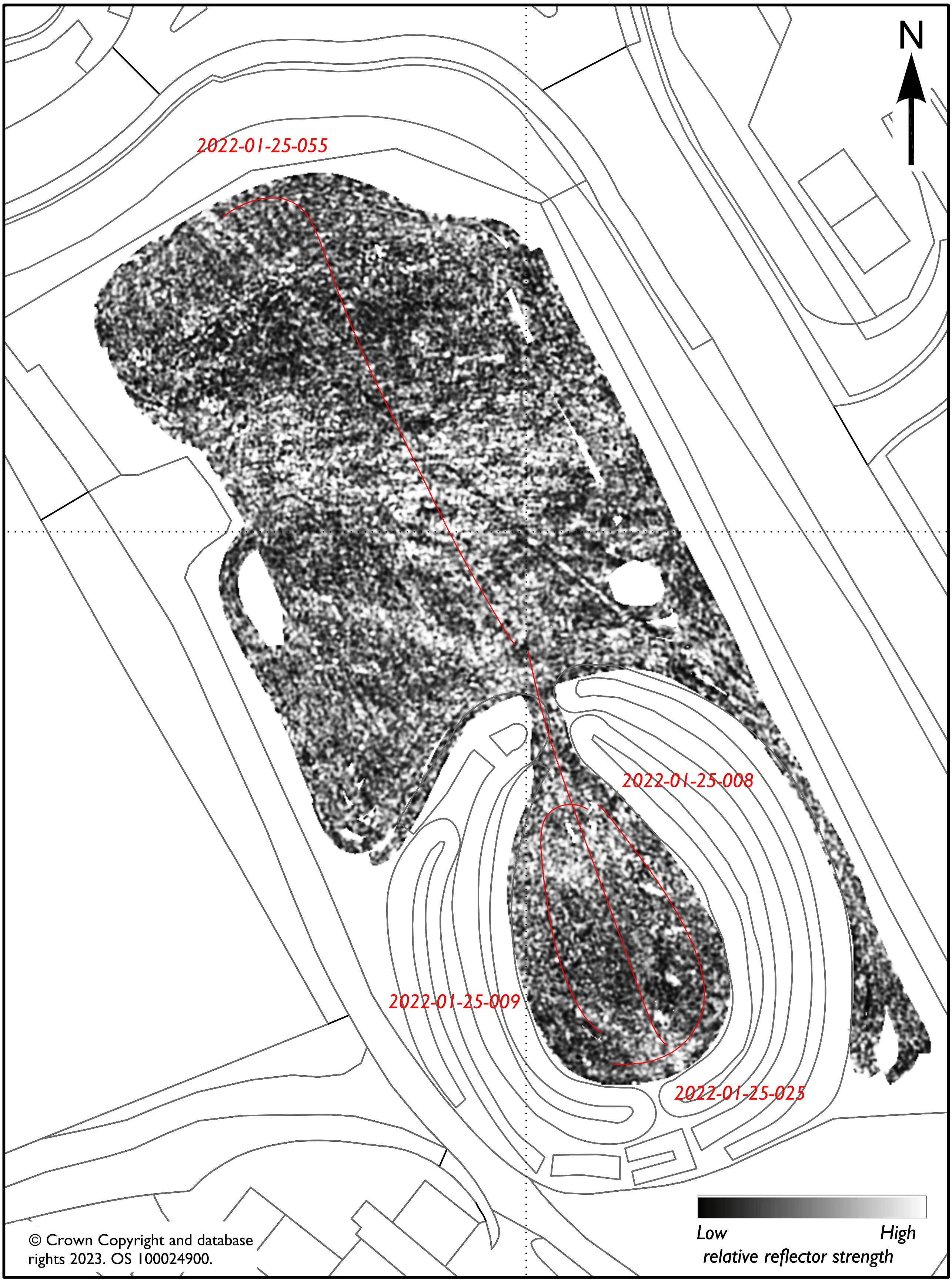

0 30m

1:750

2022-01-25-001 Location of selected GPR profiles shown on Figure 7

Geophysics Team 2023

Historic England

Figure 3

CASTILLY HENGE, LUXULYAN, CORNWALL

Location of fluxgate magnetometer and earth resistance surveys, January 2022

Geophysics Team 2023

Historic England

Figure 4

CASTILLY HENGE, LUXULYAN, CORNWALL
Location of fluxgate magnetometer survey, January 2022

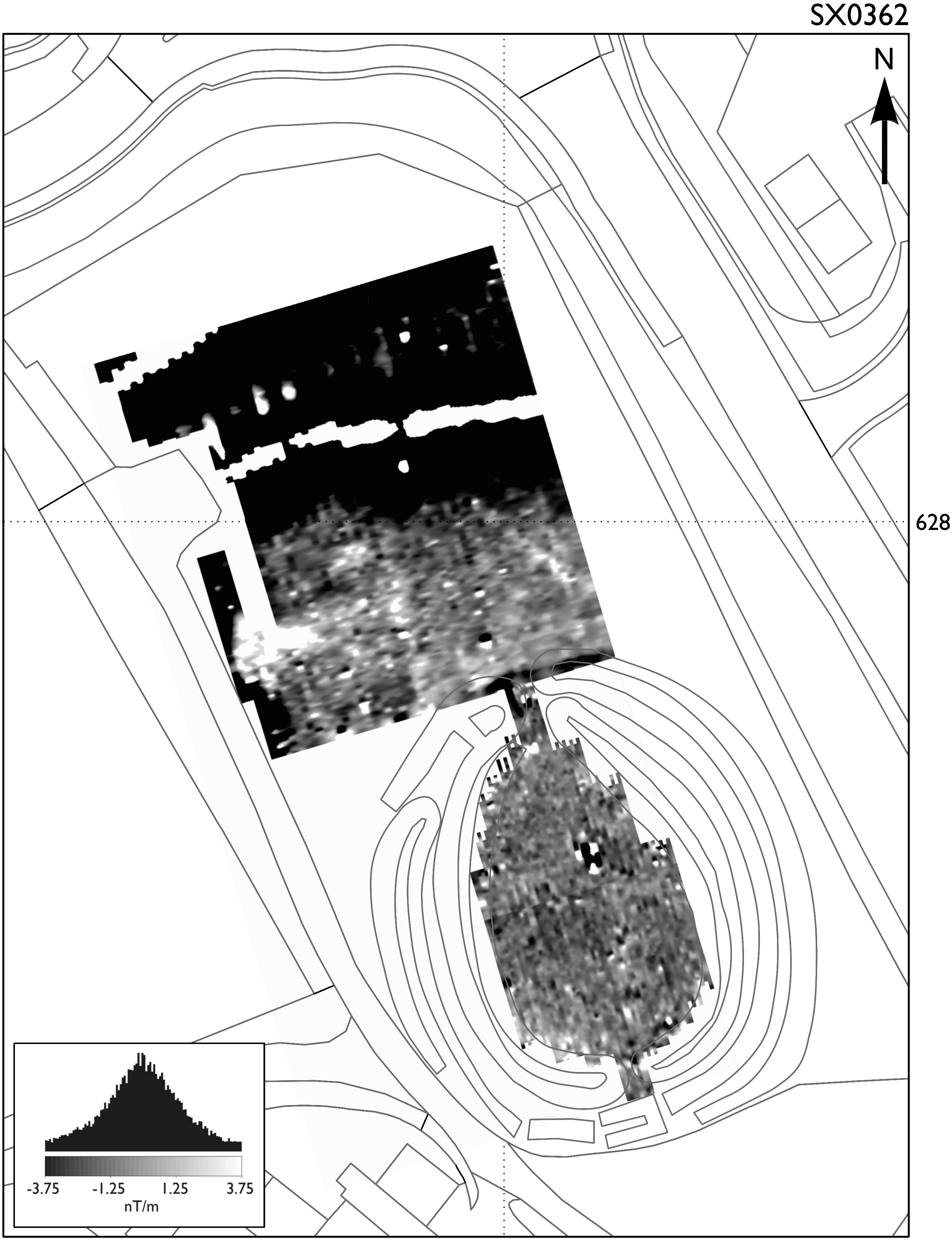

0 60m
1:750

Geophysics Team 2023

Historic England

CASTILLY HENGE, LUXULYAN, CORNWALL
Location of fluxgate magnetometer survey, January 2022

Geophysics Team 2023

Historic England

Figure 6

CASTILLY HENGE, LUXULYAN, CORNWALL
Location of earth resistance survey, January 2022

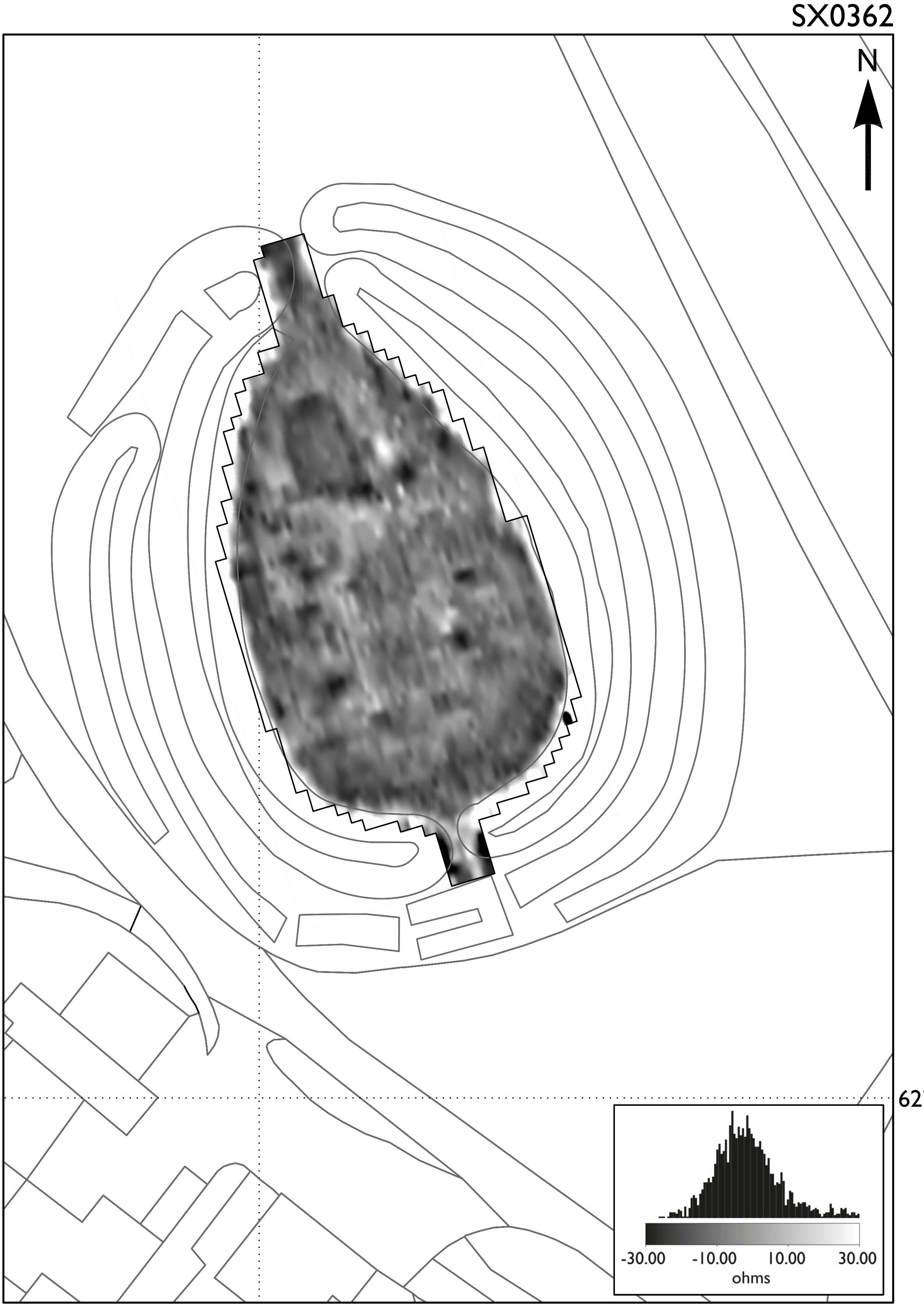

0 30m

1:500

Geophysics Team 2023

Historic England

CASTILLY HENGE, LUXULYAN, CORNWALL
Selected GPR profiles, January 2022

Figure 7

2022-01-25-008 channel 01

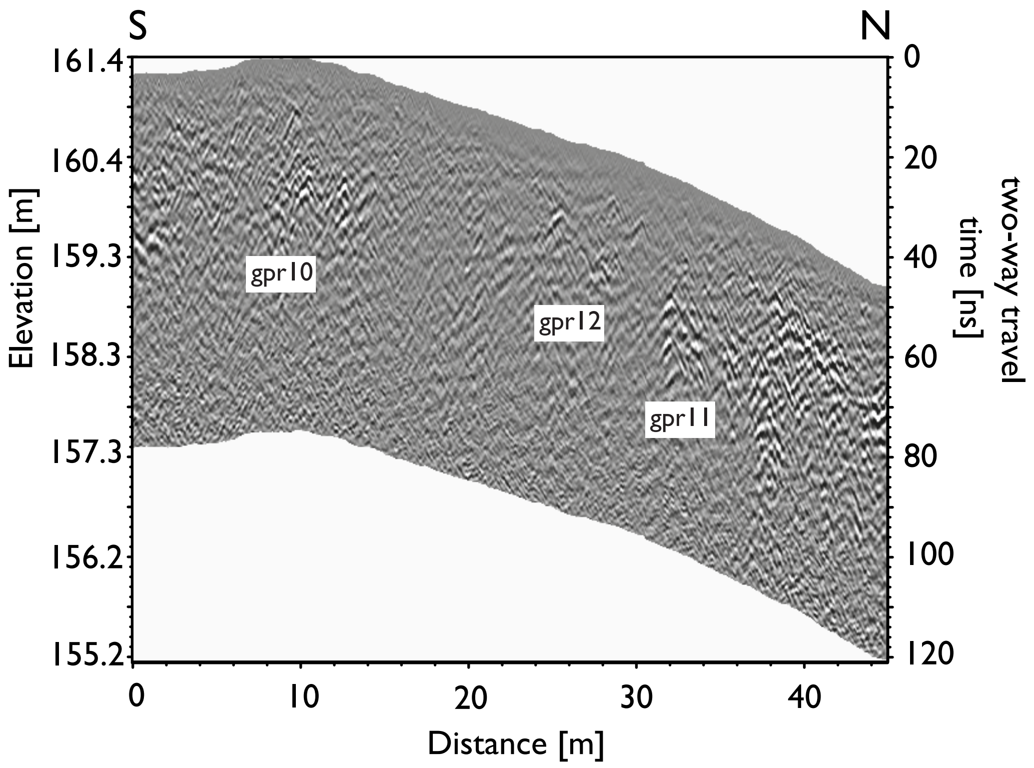

2022-01-25-009 channel 04

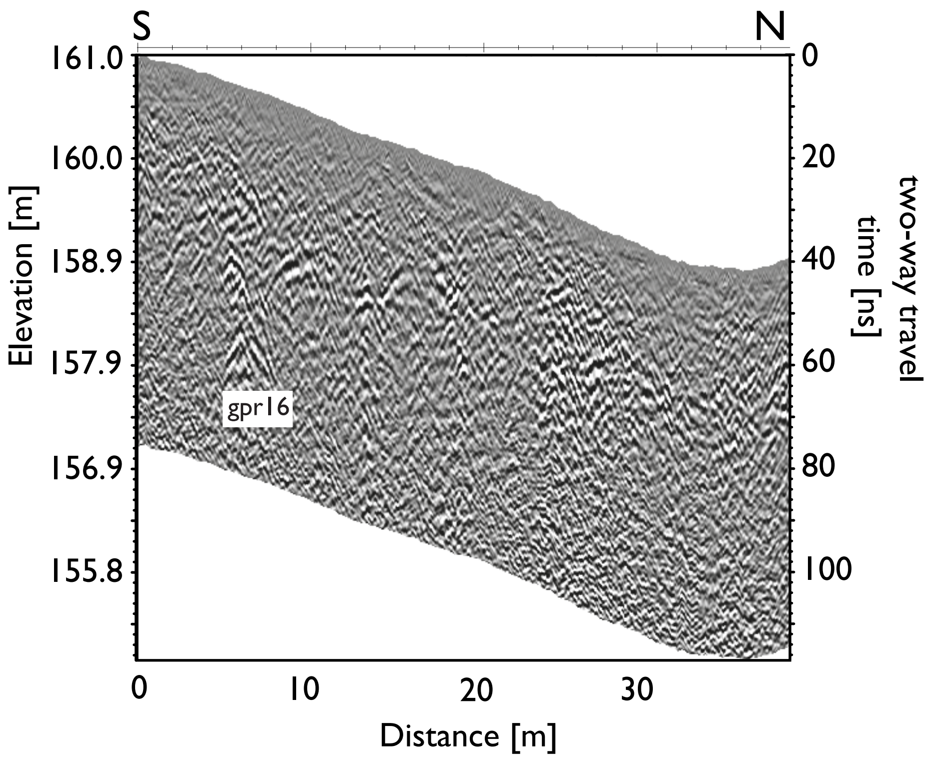

2022-01-25-025 channel 10

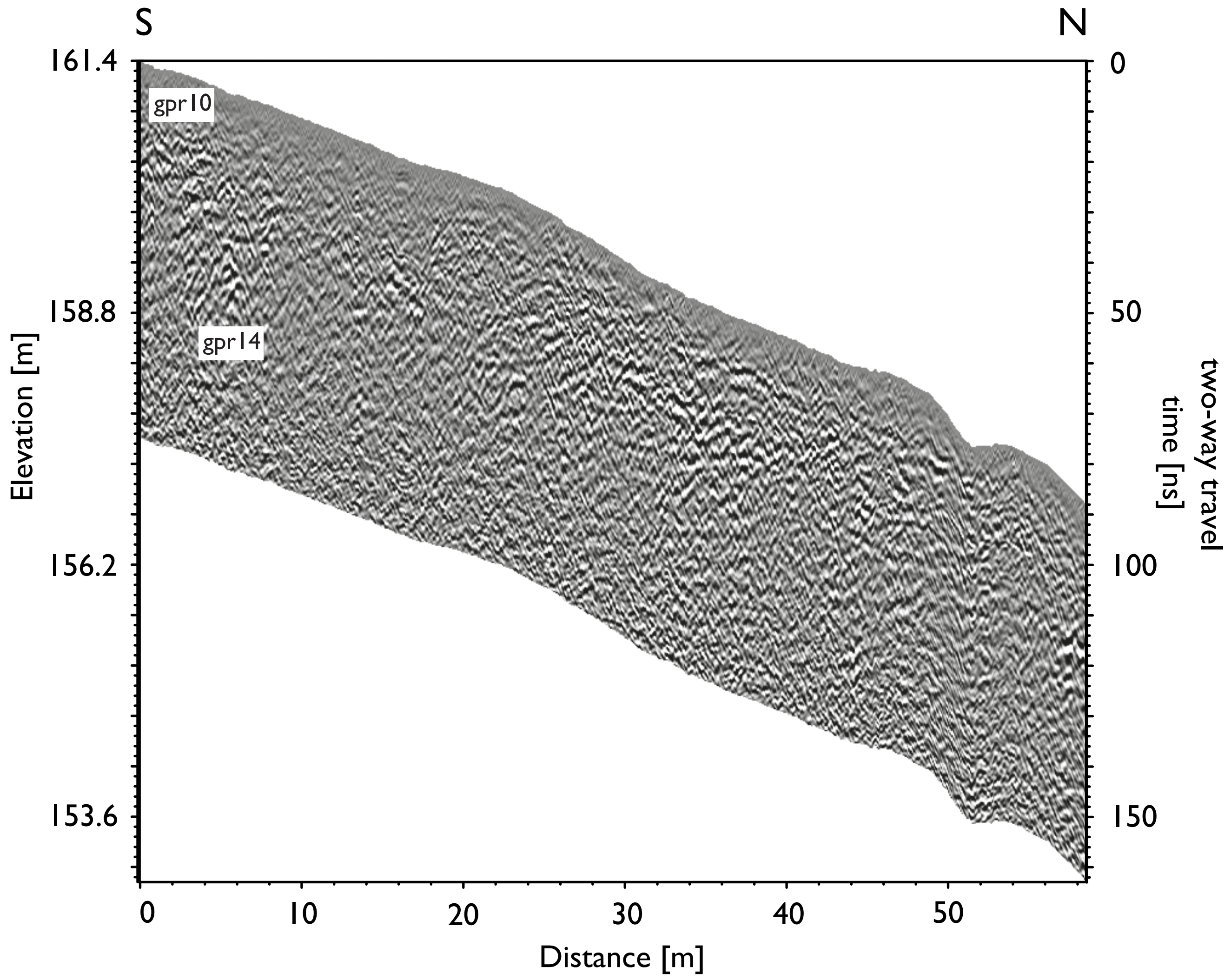

2022-01-25-055 channel 10

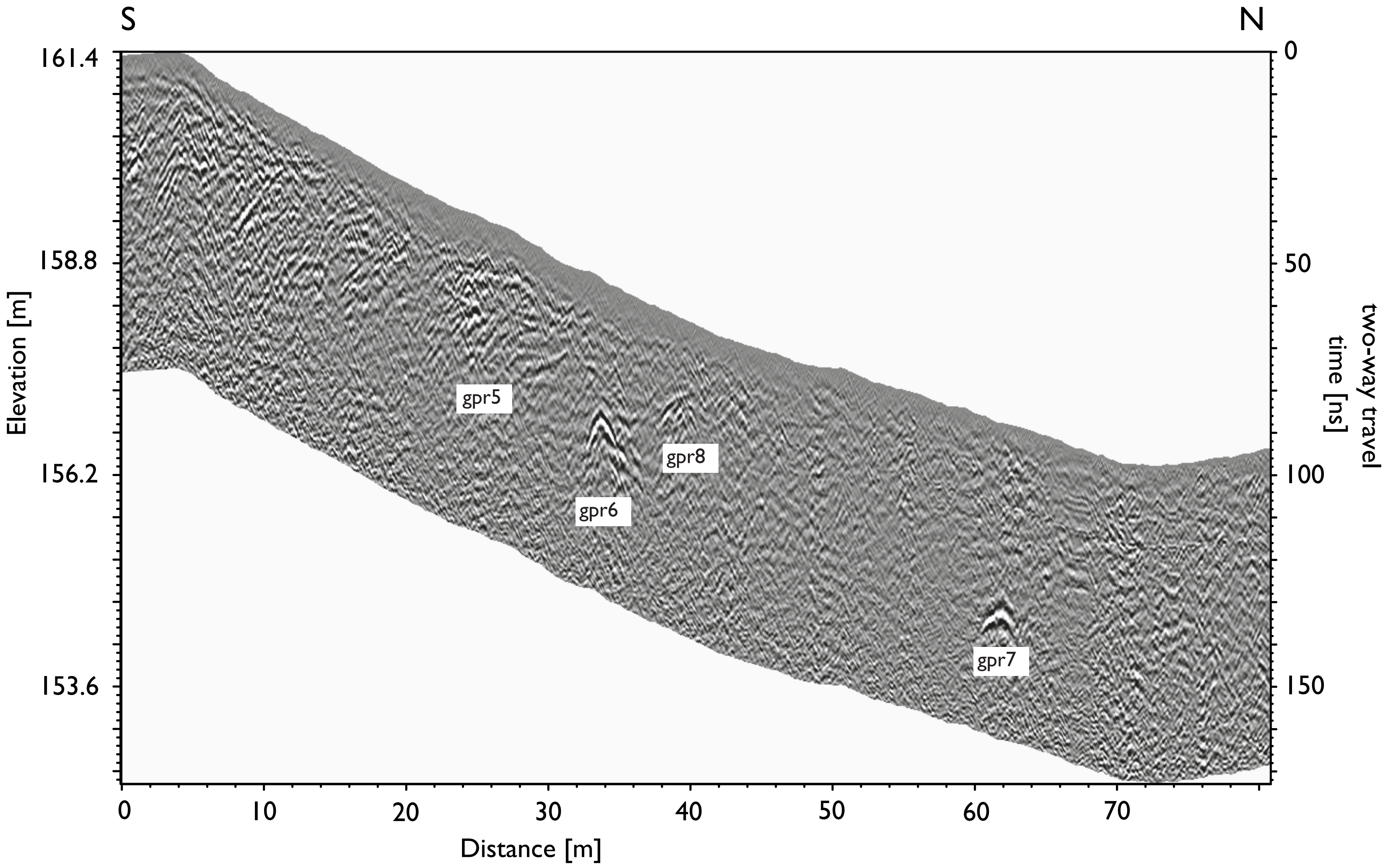

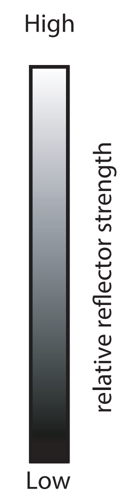

Geophysics Team 2022

Historic England

Figure 8

CASTILLY HENGE, LUXULYAN, CORNWALL
GPR amplitude time slices between 0.0 and 30.0ns (0.0 to 1.04m), January 2022

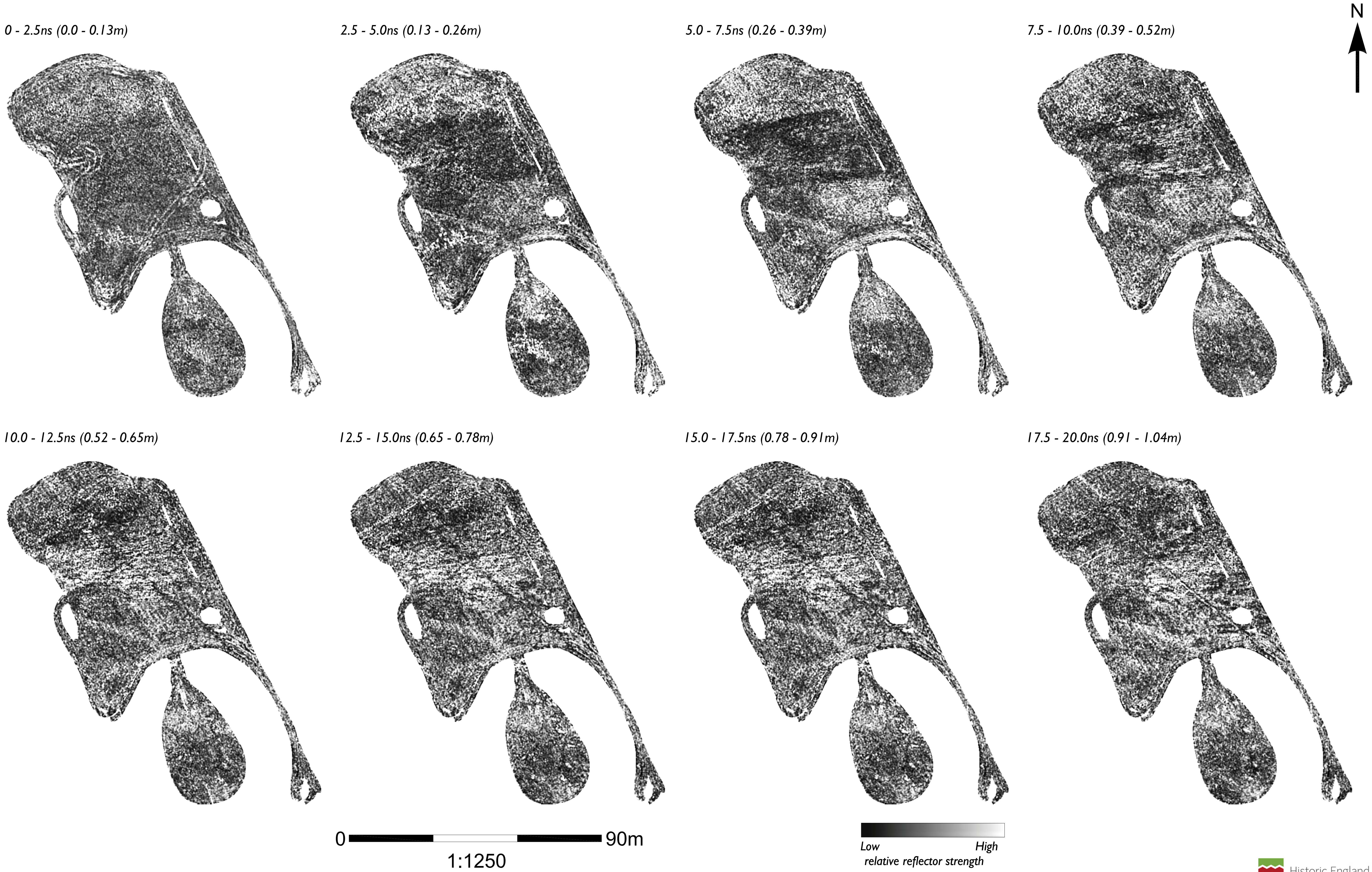

Geophysics Team 2023

Historic England

Figure 9

CASTILLY HENGE, LUXULYAN, CORNWALL
GPR amplitude time slices between 20.0 and 40.0ns (1.04 to 2.08m), January 2022

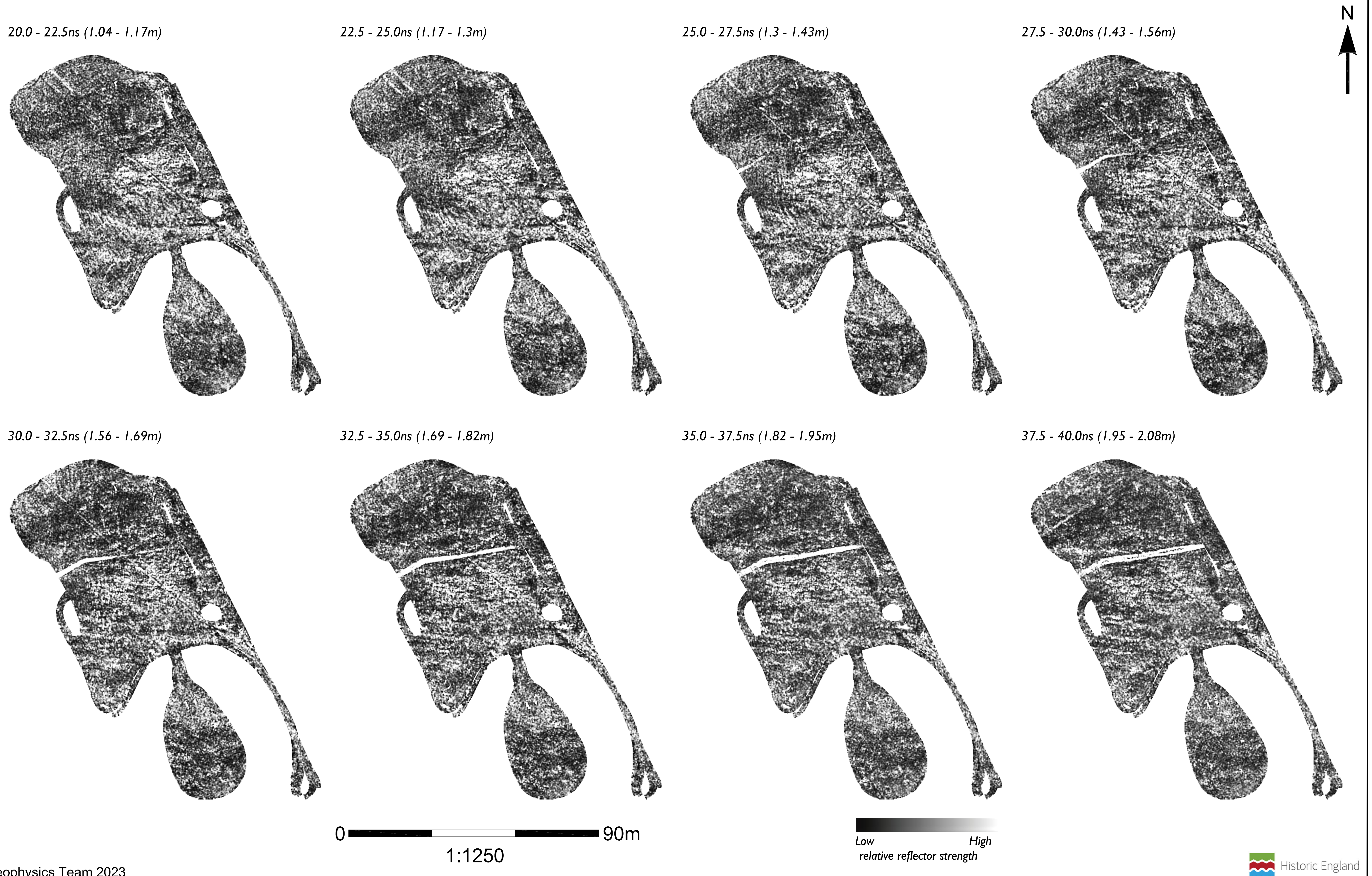

Geophysics Team 2023

Historic England

Figure 10

CASTILLY HENGE, LUXULYAN, CORNWALL
GPR amplitude time slices between 40.0 and 60.0ns (2.08 to 3.12m), January 2022

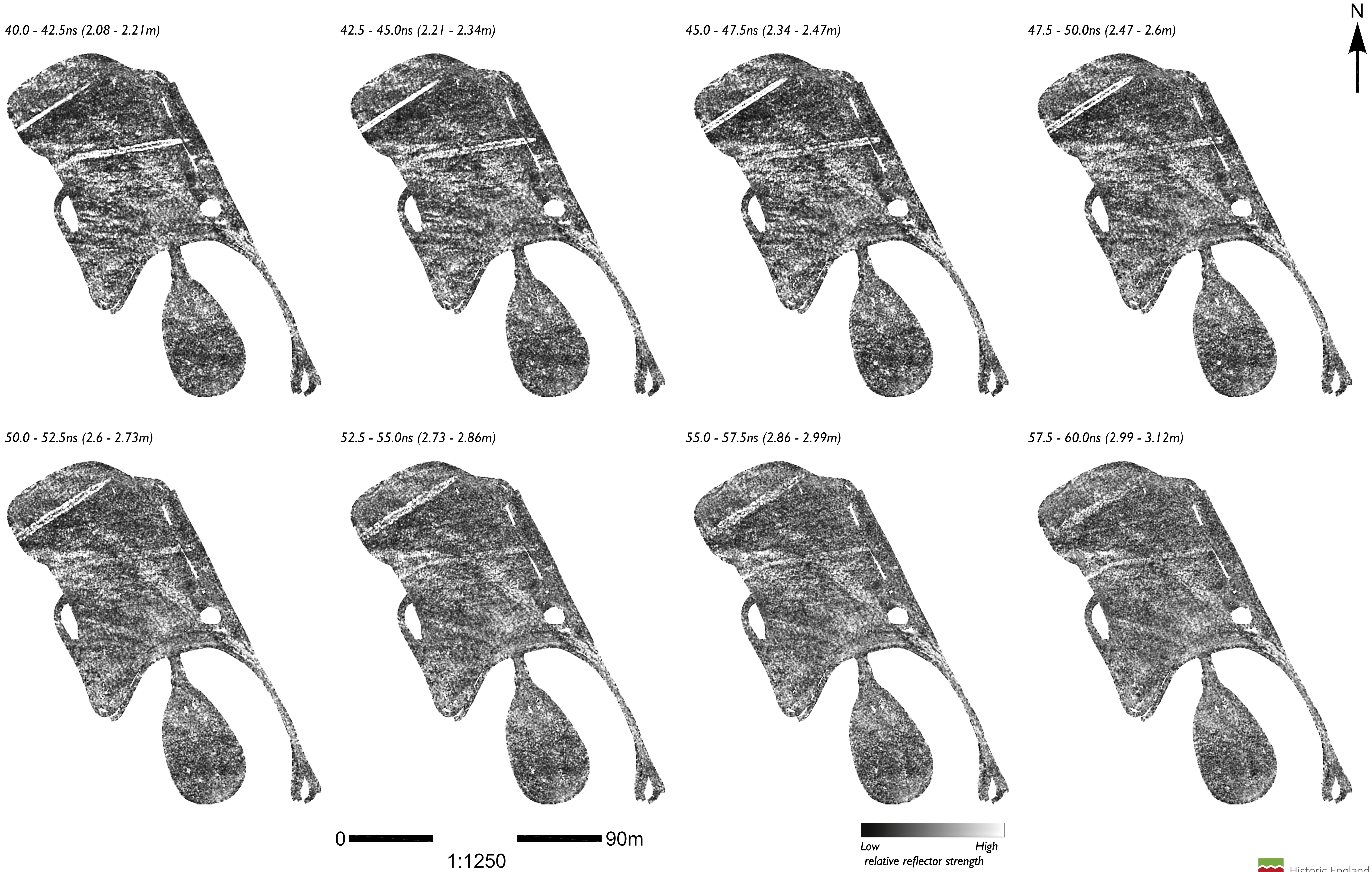

Geophysics Team 2023

Historic England

Figure 11

CASTILLY HENGE, LUXULYAN, CORNWALL
Fluxgate magnetometer survey, January 2022

(A) Trace plot of range truncated (-150/+150 nT/m) magnetometer data

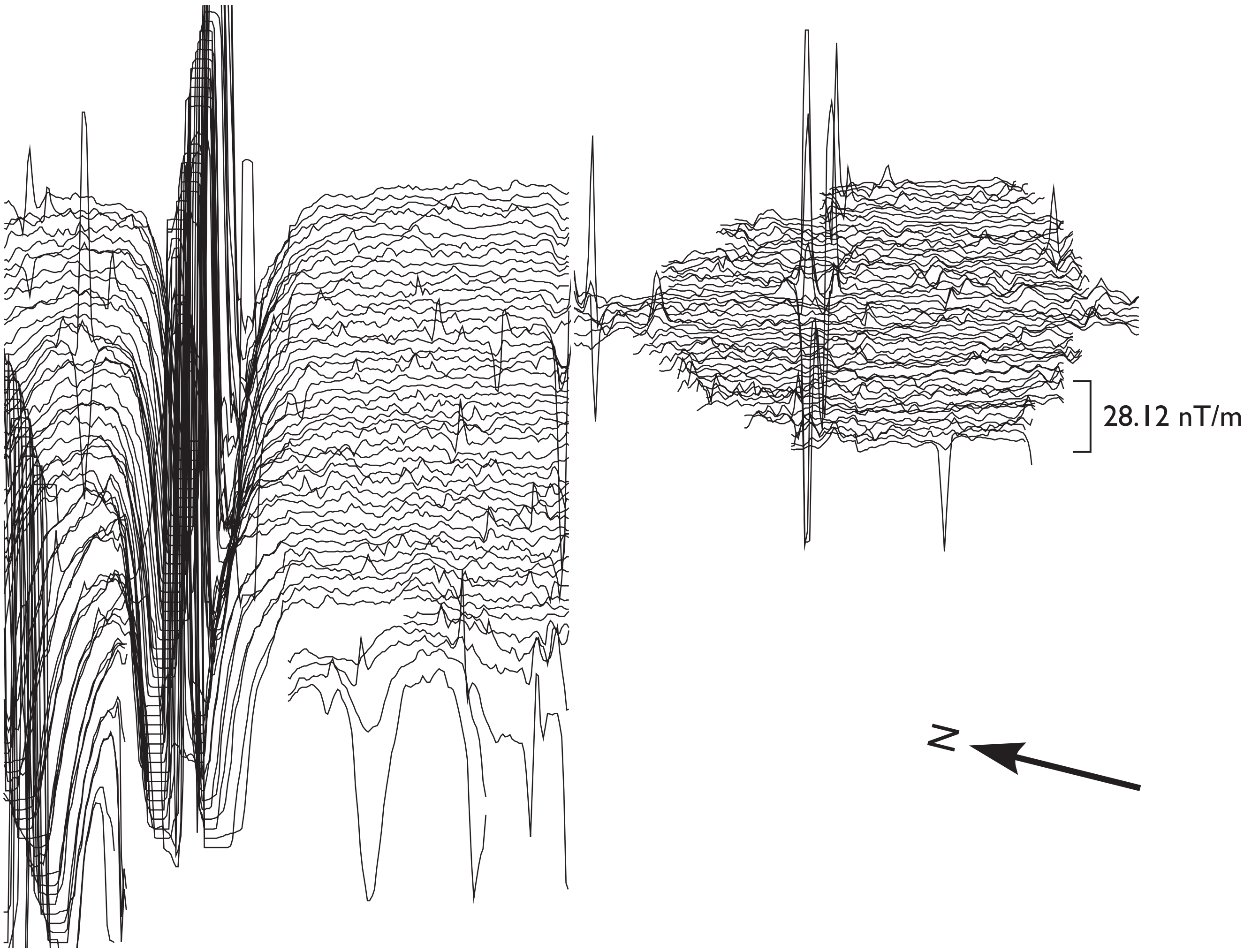

(B) Linear greyscale image of minimally processed magnetometer data

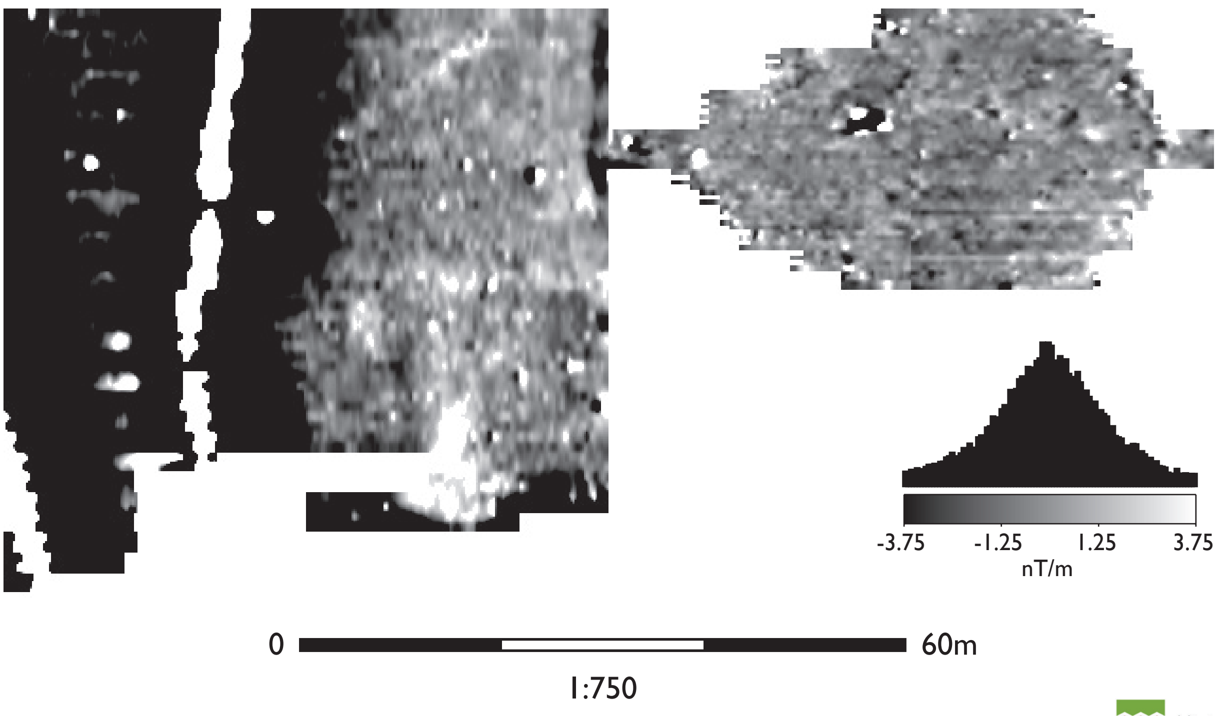

Figure 12

CASTILLY HENGE, LUXULYAN, CORNWALL
Earth resistance survey, January 2022

0.5m mobile probe separation data

(A) Trace plot of minimally processed data

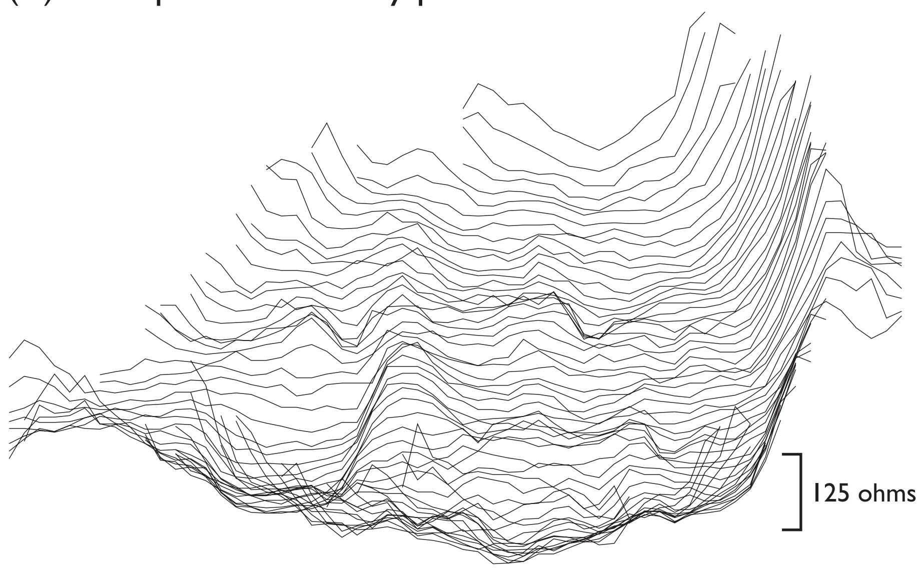

(B) Linear greyscale image of minimally processed data

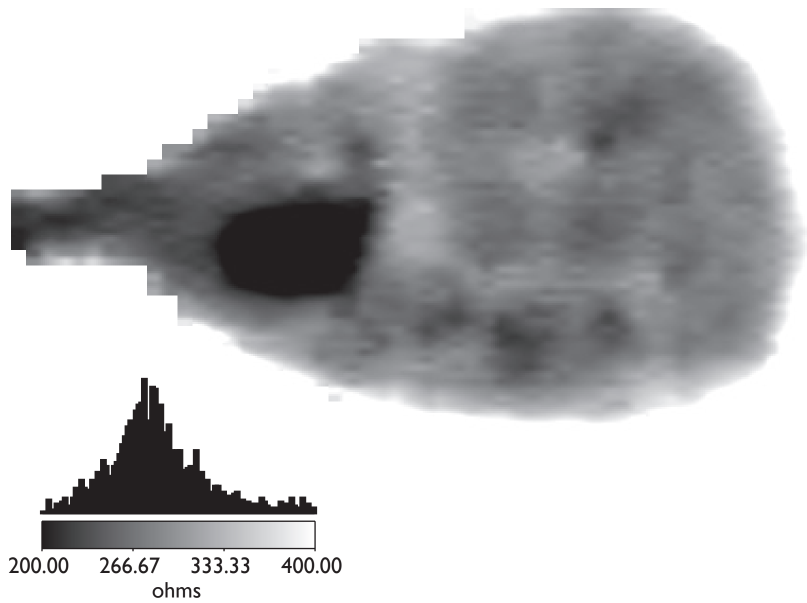

(C) Linear greyscale image of high-pass filtered data

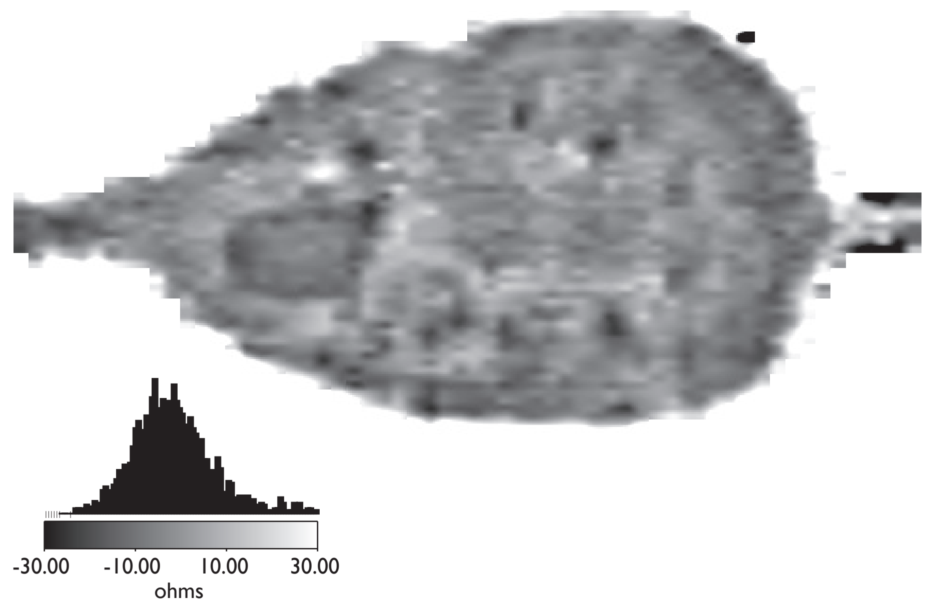

1.0m mobile probe separation data

(D) Trace plot of minimally processed data

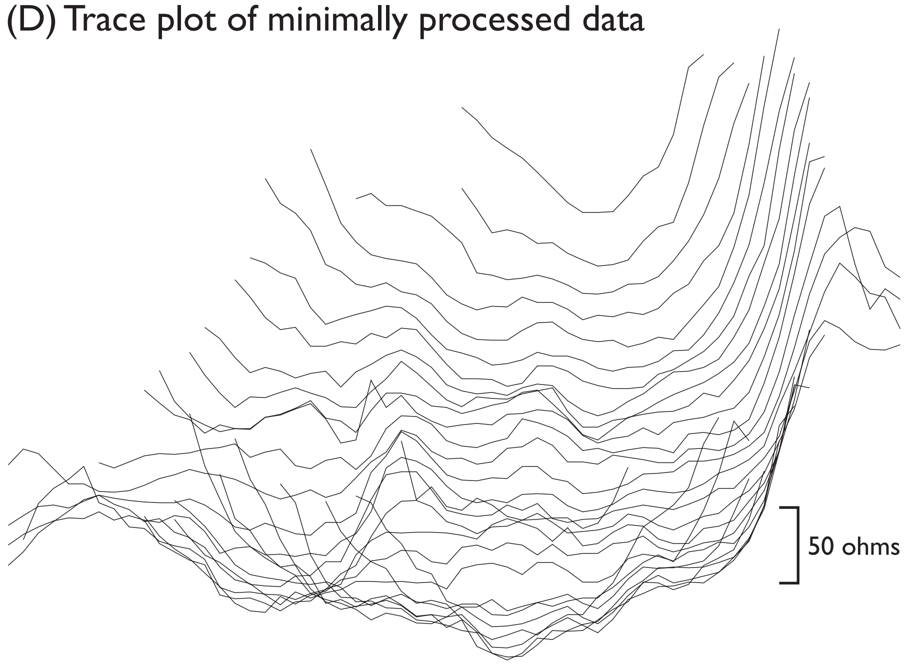

(E) Linear greyscale image of minimally processed data

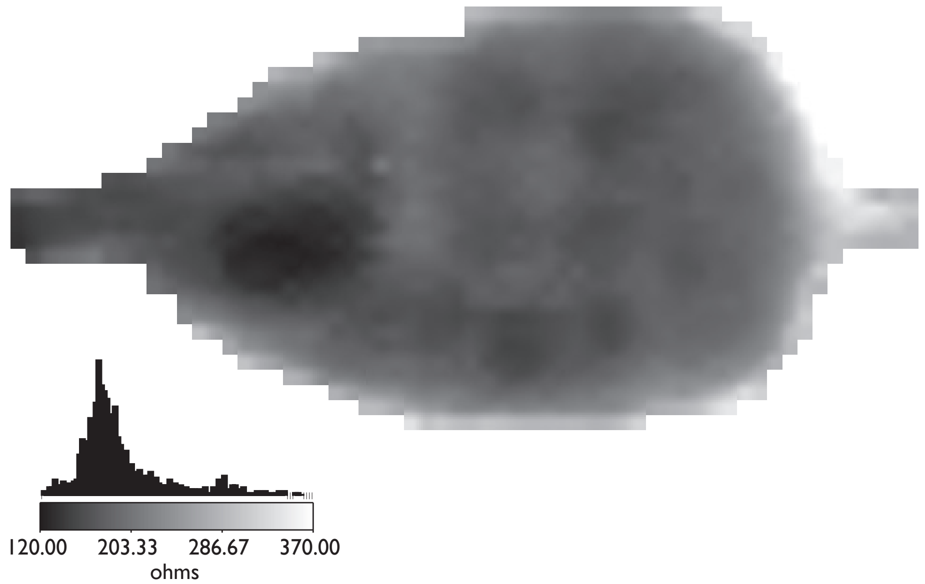

(F) Linear greyscale image of high-pass filtered data

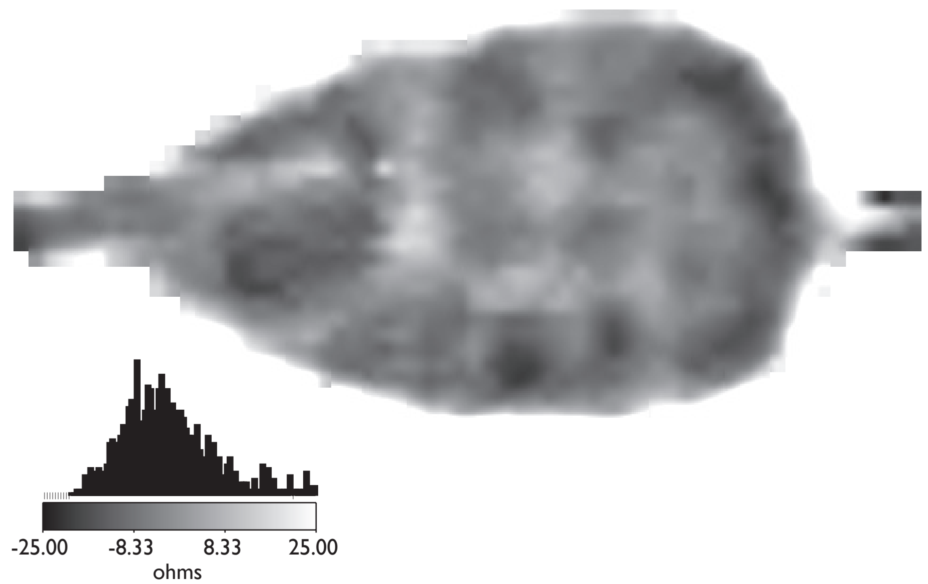

1:500

Geophysics Team 2023

Figure 13

CASTILLY HENGE, LUXULYAN, CORNWALL
Graphical summary of significant GPR anomalies, January 2022

SX0362

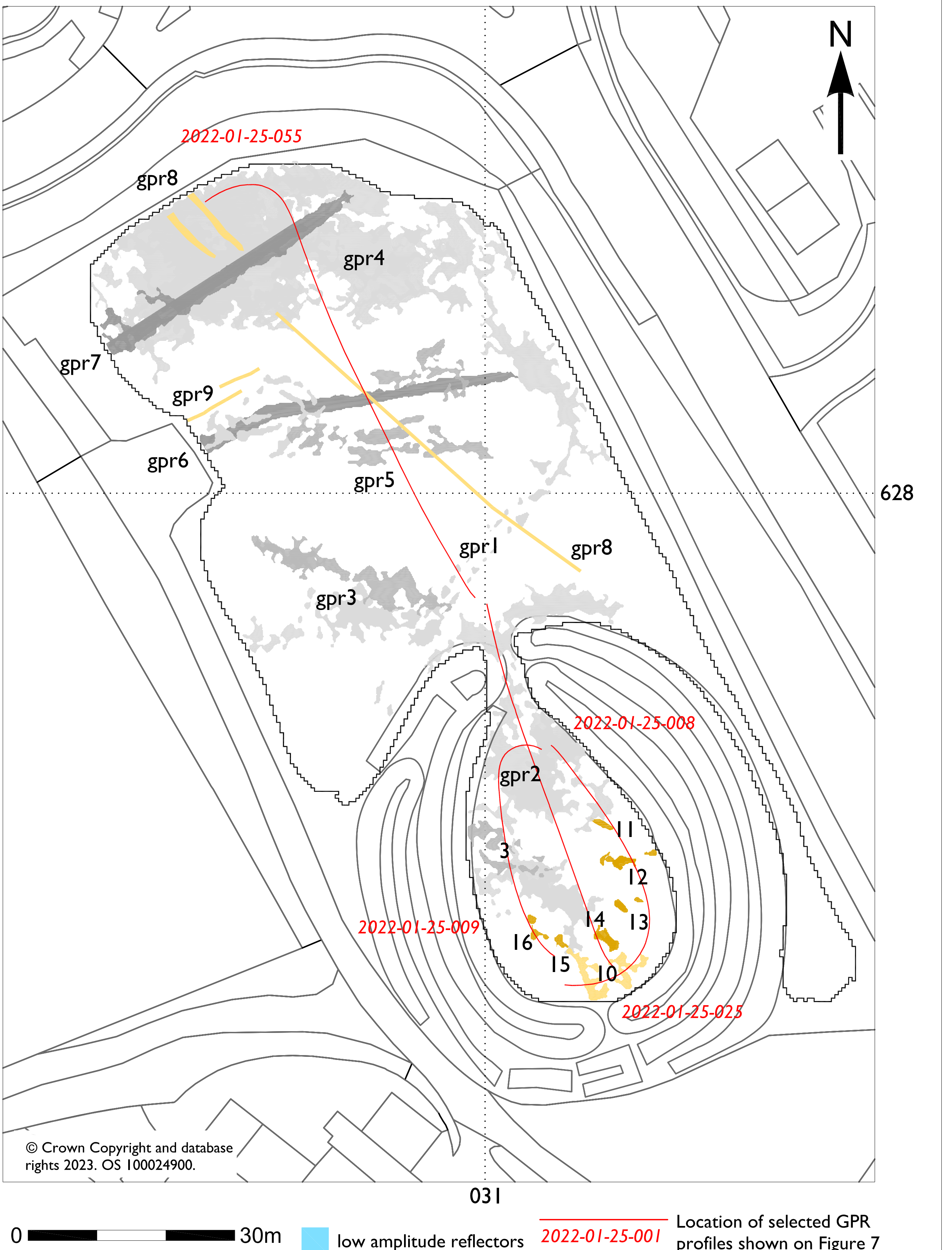

Geophysics Team 2023

Historic England

Figure 14

CASTILLY HENGE, LUXULYAN, CORNWALL
Graphical summary of significant magnetic and earth resistance anomalies, January 2022

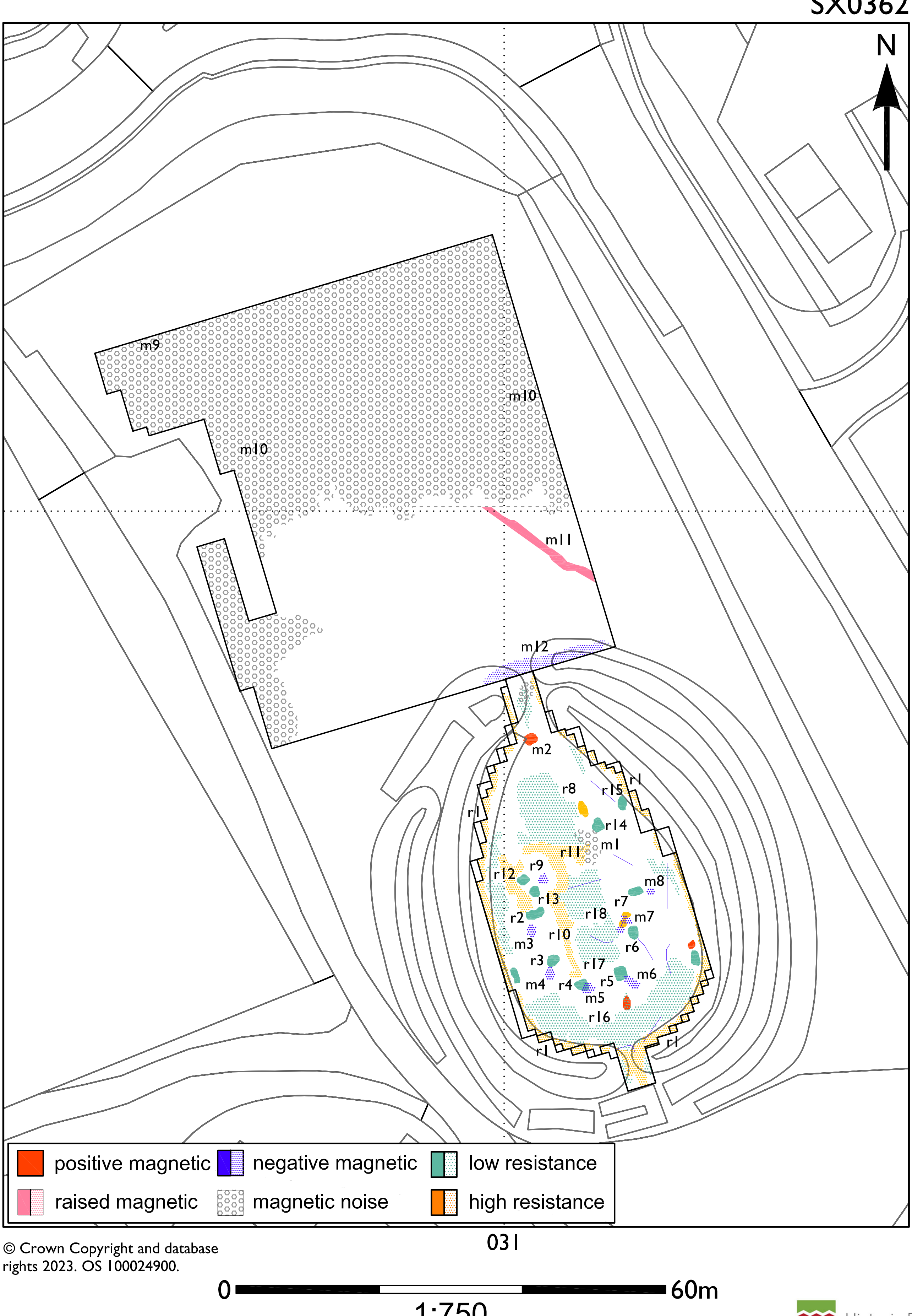

Geophysics Team 2023

Historic England

Historic England

Historic England's Research Reports

We are the public body that helps people care for, enjoy and celebrate England's historic environment.

We carry out and fund applied research to support the protection and management of the historic environment. Our research programme is wide-ranging and both national and local in scope, with projects that highlight new discoveries and provide greater understanding, appreciation and enjoyment of our historic places.

More information on our research strategy and agenda is available at HistoricEngland.org.uk/research/agenda.

The Research Report Series replaces the former Centre for Archaeology Reports Series, the Archaeological Investigation Report Series, the Architectural Investigation Report Series, and the Research Department Report Series.

All reports are available at HistoricEngland.org.uk/research/results/reports. There are over 7,000 reports going back over 50 years. You can find out more about the scope of the Series here: HistoricEngland.org.uk/research/results/about-the-research-reports-database.

Keep in touch with our research through our digital magazine *Historic England Research* HistoricEngland.org.uk/whats-new/research.

ISSN 2398-3841 (Print)
ISSN 2059-4453 (Online)